

Title:

Data collaboration for causal inference from limited medical testing and medication data

Authors and affiliations:

Tomoru Nakayama

Graduate School of Science and Technology, University of Tsukuba, Tsukuba, Japan
s2420512@u.tsukuba.ac.jp

Yuji Kawamata (Corresponding author)

Center for Artificial Intelligence Research, University of Tsukuba, Tsukuba, Japan
yjkawamata@gmail.com

Akihiro Toyoda

Graduate School of Science and Technology, University of Tsukuba, Tsukuba, Japan
s2320513@u.tsukuba.ac.jp

Akira Imakura

Center for Artificial Intelligence Research, University of Tsukuba, Tsukuba, Japan
imakura@cs.tsukuba.ac.jp

Rina Kagawa

Artificial Intelligence Research Center, National Institute of Advanced Industrial Science and Technology, Tsukuba, Japan
sonata.skazka@gmail.com

Masaru Sanuki

Faculty of Medicine, Department of Clinical Medicine, University of Tsukuba, Tsukuba, Japan
sanuki@md.tsukuba.ac.jp

Ryoya Tsunoda

Faculty of Medicine, Department of Nephrology, University of Tsukuba, Tsukuba, Japan
tsunoda@md.tsukuba.ac.jp

Kunihiro Yamagata

Faculty of Medicine, Department of Nephrology, University of Tsukuba, Tsukuba, Japan
k-yamaga@md.tsukuba.ac.jp

Tetsuya Sakurai

Center for Artificial Intelligence Research, University of Tsukuba, Tsukuba, Japan
sakurai@cs.tsukuba.ac.jp

Yukihiko Okada

Center for Artificial Intelligence Research, University of Tsukuba, Tsukuba, Japan
okayu@sk.tsukuba.ac.jp

Abstract

Observational studies enable causal inferences when randomized controlled trials (RCTs) are not feasible. However, integrating sensitive medical data across multiple institutions introduces significant privacy challenges. The data collaboration quasi-experiment (DC-QE) framework addresses these concerns by sharing “intermediate representations”—dimensionality-reduced data derived from raw data—instead of the raw data. While the DC-QE can estimate treatment effects, its application to medical data remains unexplored.

This study applied the DC-QE framework to medical data from a single institution to simulate distributed data environments under independent and identically distributed (IID) and non-IID conditions. We propose a novel method for generating intermediate representations within the DC-QE framework. Experimental results demonstrated that DC-QE consistently outperformed individual analyses across various accuracy metrics, closely approximating the performance of centralized analysis. The proposed method further improved performance, particularly under non-IID conditions.

These outcomes highlight the potential of the DC-QE framework as a robust approach for privacy-preserving causal inferences in healthcare. Broader adoption of this framework and increased use of intermediate representations could grant researchers access to larger, more diverse datasets while safeguarding patient confidentiality. This approach may ultimately aid in identifying previously unrecognized causal relationships, support drug repurposing efforts, and enhance therapeutic interventions for rare diseases.

Keywords: Propensity score matching; Privacy-preserving causal inference; Data collaboration framework; Distributed data

Introduction

Randomized controlled trials (RCTs) represent the gold standard for causal inference. However, conducting RCTs in epidemiological and medical contexts poses significant challenges due to ethical and financial constraints, particularly when timely interventions are required. These limitations render observational studies a valuable alternative for deriving causal inferences[1–3]. However, such studies rely on large datasets to ensure reliable outcomes, yet sharing raw data in sensitive domains like medicine and finance remains challenging due to privacy concerns[4–7]. Hence, considerable research has focused on developing privacy-preserving concerns.

Federated Learning (FL) is one such approach that has been widely adopted in machine learning tasks[8]. FL achieves privacy preservation by sharing models instead of raw data. This methodology has garnered significant attention in the medical field[9], with numerous studies demonstrating its utility[10–12]. Specifically, Imakura and Sakurai introduced data collaboration (DC) analysis as a model non-sharing FL framework[13]. DC analysis facilitates data integration across horizontal and vertical dimensions without requiring continuous communication with external entities. An example of its application in healthcare includes collaboration between a hospital and a city to develop a model for diabetes prediction[14].

Kawamata et al. extended DC analysis by proposing the data collaboration quasi-experiment (DC-QE), a framework designed for causal inference[15]. DC-QE enables treatment effect estimation from distributed data while addressing covariate biases between treatment and control groups by combining DC analysis with propensity score matching[16]. The increasing availability of diverse healthcare datasets (e.g., health checkup records, electronic medical records, and imaging data) coupled with the frequent use of propensity score matching in actual cohort studies[17–20] underscores the potential of DC-QE in the medical field. However, the potential of DC-QE remains untested with medical data because it has been applied exclusively to artificial datasets and labor training programs.

This study evaluated the effectiveness of DC-QE using medical data. Specifically, the study focused on assessing the DC-QE framework for estimating the effect of uric acid-lowering s on reducing uric acid levels. Kawamata et al.[15] conducted experiments under IID data distribution scenarios. Therefore, we initiated experiments under IID conditions. Subsequently, we conducted experiments under non-IID conditions to extend the evaluation to more generalized settings, where local data distributions were non-identically independently distributed. Additionally, we propose a method for generating intermediate representations, a dimensionality reduction technique aimed at enhancing the performance of DC-QE. The main contributions of this study are as follows:

- A practical dimensionality reduction method for DC-QE is proposed.
- The effectiveness of DC-QE on medical data partitioned into IID and non-IID settings is demonstrated for the first time.
 - Conducting full collaboration among all institutions using DC-QE under IID settings resulted in performance surpassing individual analyses across all evaluation metrics.
 - Selecting appropriate intermediate representations enabled DC-QE to outperform individual analyses across multiple evaluation metrics under non-IID settings.

Data and methodology

The handling of medical data was approved by the Ethical Review Committee for Clinical Research of the University of Tsukuba Hospital (permission number: R04-147). All procedures involving human participants were in accordance with the ethical standards of the 1964 Helsinki Declaration and its later amendments. Informed consent was not obtained for this study because it did not involve intervention

or the collection of new samples. Instead, opt-outs were obtained by posting a written explanation of the study in the hospital and on the website, including the possibility of refusing to allow medical information to be used in the study, according to the Ethical Guidelines for Medical and Biological Research Involving Human Subjects established by the Ministry of Health, Labor and Welfare of Japan (<https://www.mhlw.go.jp/content/001077424.pdf>, in Japanese).

Study design and data settings

The study used examination and prescription history data from Tsukuba University Hospital, spanning 2014 to 2020. The examination history dataset included blood tests and urinalysis data, while the prescription history dataset documented medications prescribed to patients during this period.

The experiment focused on verifying the effectiveness of uric-lowering agents (ULAs), specifically allopurinol and febuxostat (hereafter, Target ULAs), in reducing serum uric acid (SUA) levels. Covariates were selected based on the study by Chou et al.[21]. Given that previous studies have demonstrated a significant reduction in SUA levels within two weeks of Target ULA administration[22–24], this study examined reductions in SUA levels between two weeks and four weeks following prescription. Although Chou et al. included allopurinol, febuxostat, and benzbromarone as treatment targets, the present study excluded benzbromarone due to insufficient sample size in the dataset.

The exclusion criteria for study subjects were as follows:

- **(i)** Age < 20 or > 100 years.
- **(ii)** History of Target ULAs prescriptions prior to July 2014.
- **(iii)** Use of multiple ULAs during the observation period.
- **(iv)** Absence of baseline or follow-up SUA data.
- **(v)** Treatment-to-follow-up SUA test interval shorter than two weeks or longer than one month.
- **(vi)** Missing values for over half of the covariates, excluding prescription history.

Features with missing values in more than half of the instances were removed after applying criterion (v). Criterion (iii) functioned as a preprocessing step to exclude the influence of medications other than the target ULAs on SUA levels. The ULAs considered for criterion (iii) included allopurinol, febuxostat, topiroxostat, benzbromarone, probenecid, dotinurad, and rasburicase. After preprocessing, missing values were imputed using the median values. Fig. 1 illustrates the preprocessing workflow, and Table 1 provides a summary of the statistical properties of the dataset after preprocessing.

The original dataset lacked values for the estimated glomerular filtration rate (eGFR), which was calculated using the following equation: $eGFR = 194 \times SCr^{-1.094} \times Age^{-0.287} \times sex$, where *Age* denotes the patient's age, *SCr* refers to the serum creatinine level, and *sex* was assigned a value of 1 for males and 0.739 for females[25]. Baseline eGFR values were computed using the most recent laboratory results available prior to treatment for the treatment group and prior to uric acid measurement for the control group. Chronic kidney disease (CKD) stages were categorized based on eGFR values into the following intervals: >90, 60–90, 30–60, 15–30, and <15 mL/min/1.73 m².

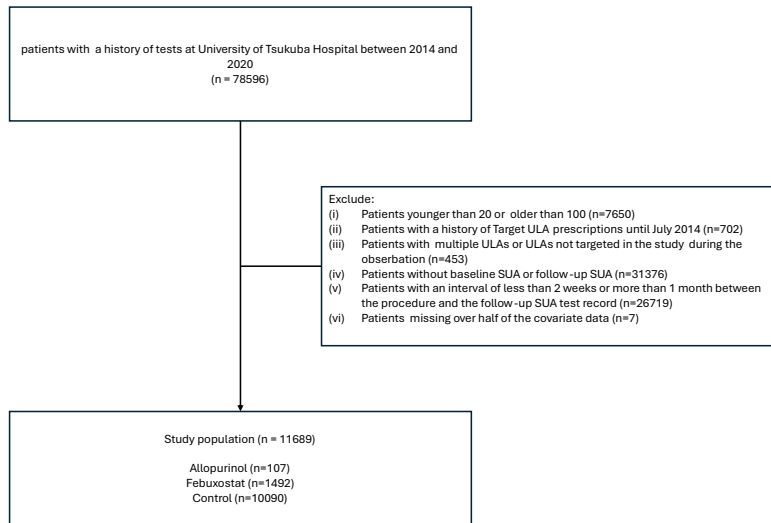


Fig. 1. Preprocessing flowchart, where n indicate the number of samples.

Table 1. Basic statistics after preprocessing.

Sample size	unit	Control n=10090		Allopurinol n=107		Febuxostat n=1492	
		N	%	N	%	N	%
Diuretic	-	33	0.33	7	6.54	86	5.76
Beta-adrenergic antagonist	-	167	1.66	15	14.02	109	7.31
Renin-angiotensin system inhibitor	-	182	1.80	19	17.76	191	12.80
Antipurine	-	9	0.09	2	1.87	12	0.80
Alkalizer	-	174	1.72	5	4.67	153	10.25
Nonsteroidal anti-inflammatory drug	-	259	2.57	9	8.41	105	7.04
Aspirin	-	10	0.10	2	1.87	9	0.60
Corticosteroid	-	422	4.18	13	12.15	257	17.23
Colchicine	-	2	0.02	0	0.00	5	0.34
CKD stage	1	4056	40.20	8	7.48	189	12.67
	2	2483	24.61	19	17.76	233	15.62
	3	2777	27.52	55	51.40	558	37.40
	4	341	3.38	6	5.61	234	15.68
	5	431	4.27	18	16.82	278	18.63
		mean	std	mean	std	mean	std
High-density lipoprotein cholesterol	mg/dl	52.55	17.20	49.03	16.10	43.98	15.77
Hemoglobin A1c	%	6.16	1.38	6.05	1.13	6.09	1.10
eGFR	g/dl	86.61	49.99	46.51	28.62	48.80	37.34
Albumin	mg/dl	3.83	0.69	3.79	0.74	3.59	0.76
Creatinine	mg/dl	1.01	1.41	1.91	2.26	2.06	2.38
Triglycerides	mg/dl	134.82	116.51	163.46	113.58	157.02	127.13
Serum uric acid	mg/dl	5.09	1.77	6.01	2.32	7.00	2.70
Age	-	58.09	17.47	65.57	13.37	62.12	15.03
Sex	-	0.52	0.50	0.16	0.37	0.30	0.46
Hemoglobin	g/dl	12.59	2.26	12.43	2.59	11.38	2.65
Urine pH	-	6.50	0.79	6.30	0.90	6.25	0.75
Urine occult blood	-	0.76	1.30	0.65	1.13	0.96	1.33

Data collaboration quasi-experiment

The DC-QE framework employed two distinct roles: data users and analysts. Users provided data, while analysts were responsible for processing and analyzing the shared information. The algorithm comprised three stages: Each user retained a private dataset $X_k \in \mathbb{R}^{n_k \times m}$, a treatment variable Z_k , and an outcome variable Y_k , where k denotes the identifier of a user, n_k represents the number of samples of user k , and m indicates the number of covariates.

Instead of sharing raw data X_k , users transform their datasets into intermediate representations suitable for sharing. The intermediate representations provided by users were integrated by the analyst into a unified collaborative representation that enabled the construction of a propensity score model. The analyst estimated the propensity scores and applied the matching results to compute the average treatment effect on the treated $\tau_{ATT}^{DC-QE(PSM)}$ using the collaborative representation.

The above steps outline the DC-QE process, facilitating collaborative data analysis while maintaining privacy. This study specifically examined horizontal data partitioning scenarios. Further algorithmic details can be found in the work of Kawamata et al.[15].

First step

In the first step, each user generated an intermediate representation of their dataset and shared it with the analyst. A common dataset, called anchor data $X^{anc} \in \mathbb{R}^{r \times m}$, was required for constructing intermediate representations, where r denotes the number of samples. Anchor data can be derived from publicly available or basic statistical datasets using techniques such as random sampling, low-rank approximation, or SMOTE[26,27]. These anchor data were essential for creating collaborative representations.

Each user produced an intermediate representation \tilde{X}_k using their dataset X_k and applied a transformation function f_k to X_k . The intermediate representations are expressed as follows:

$$\tilde{X}_k = f_k(X_k) \in \mathbb{R}^{n_k \times \tilde{m}_k} \quad (1)$$

$$\tilde{X}_k^{anc} = f_k(X^{anc}) \in \mathbb{R}^{r \times \tilde{m}_k} \quad (2)$$

where f_k represents a row-wise dimensionality reduction function, which can include methods such as principal component analysis (PCA)[28], linear discrimination analysis[29], and locality-preserving projections[30]. The number of dimensions after reduction, \tilde{m}_k , was determined independently by each user. Once the intermediate representations were constructed, the representations $\tilde{X}_k, \tilde{X}_k^{anc}$, along with the treatment Z_k , and outcome Y_k , were shared with the analyst.

Second step

In the subsequent step, the analyst constructed collaborative representations from the intermediate representations provided by the users. A transformation function must be applied to standardize these representations for integrated analysis because the dimensions of the shared intermediate representations may vary across users. The transformation function satisfied the following equation for all k :

$$g_k(\tilde{X}_k^{anc}) \approx g_{k'}(\tilde{X}_{k'}^{anc}) \in \mathbb{R}^{r \times \tilde{m}} \quad (k \neq k') \quad (3)$$

where \tilde{m} denotes the dimension of the collaborative representation. Assuming g_k is a linear transformation, the transformation function g_k for user k can be defined as follows:

$$\tilde{X}_k = g_k(\tilde{X}_k) = \tilde{X}_k G_k \in \mathbb{R}^{n_k \times \tilde{m}} \quad (4)$$

where G_k represents the linear transformation matrix. G_k can be approximated using a singular value decomposition (SVD). Let the concatenated matrix of \tilde{X}_i^{anc} be expressed as:

$$[\tilde{X}_1^{anc}, \tilde{X}_2^{anc}, \dots, \tilde{X}_c^{anc}] = [U_1, U_2] \begin{bmatrix} \Sigma_1 & & \\ & \Sigma_2 & \end{bmatrix} \begin{bmatrix} V_{11}^T & \dots & V_{c1}^T \\ V_{12}^T & \dots & V_{c2}^T \end{bmatrix} \quad (5)$$

Then, G_k is obtained as follows:

$$G_k = (\tilde{X}_k^{anc})^\dagger U_1 C \quad (6)$$

where \dagger denotes the Moore–Penrose pseudoinverse and $C \in \mathbb{R}^{\hat{m} \times \hat{m}}$ represents a regular matrix, such as the identity matrix. The collaborative representation using the computed G_k is expressed as follows:

$$\check{X} = \begin{bmatrix} \check{X}_1 \\ \check{X}_2 \\ \vdots \\ \check{X}_c \end{bmatrix} = \begin{bmatrix} \check{X}_1 G_1 \\ \check{X}_2 G_2 \\ \vdots \\ \check{X}_c G_c \end{bmatrix} \in \mathbb{R}^{n \times \tilde{m}} \quad (7)$$

Third step

In the third step, a model was developed to estimate the propensity score based on the collaborative representation, and the treatment effect was calculated using propensity score matching. The propensity score α is defined as follows:

$$\alpha_i = Pr(z_i = 1 | \check{x}_i) \quad (8)$$

where \check{x}_i represents the collaborative representation of covariates for subject i . Logistic regression is commonly employed to estimate propensity scores. The matching pair $pair^{DC-QE}(i)$ for subject i was determined using these estimated propensity scores in the DC-QE framework. The treatment effect is estimated using the following equation:

$$\hat{\tau}_{ATT}^{DC-QE(PSM)} = \frac{1}{n} \sum_{i \in \mathbb{N}_T} (y_i - y_{pair^{DC-QE}(i)}) \quad (9)$$

Dimensionality reduction method for DC-QE

The matching performance in DC-QE was influenced by the dimensionality-reduction method. Therefore, we propose a bootstrap-based dimensionality reduction method, inspired by the work of Imakura et al.[31], to enhance this performance. This approach estimates multiple parameters via the bootstrap method and constructs a subspace from the resulting values. Let β_k denote the model parameters that estimate the propensity scores computed from the subspace $\mathcal{S}_k = \mathcal{R}(F_k G_k) \subset \mathcal{R}(F_k)$. If the range $\mathcal{R}(F_k)$ includes the true estimator derived from centralized analysis (CA), it can also be approximated through DC-QE. The bootstrap-based method provides a robust alternative because β_k , estimated from the dataset of each user, approximates the centralized true estimator. Given a sampling ratio $0 < p < 1$, user k randomly extracted pn_k samples from their total dataset of size n_k . The model parameters were estimated through this sampling process, which was repeated \tilde{m}_{BS} times to generate $\beta_1, \beta_2, \dots, \beta_{\tilde{m}_{BS}}$. The constructed parameters formed the matrix: $F_k^{BS} = [\beta_1, \beta_2, \dots, \beta_{\tilde{m}_{BS}}] \in \mathbb{R}^{m_k \times \tilde{m}_{BS}}$. This matrix which was combined with another dimensionality reduction function $F^{DR} \in \mathbb{R}^{m_k \times \tilde{m}_{DR}}$, generated using alternative methods, where $\tilde{m} = \tilde{m}_{BS} + \tilde{m}_{DR}$. The combined bootstrap-based dimensionality reduction function F_k is defined as follows:

$$F_k = [F_k^{DR}, F_k^{BS}] E_k, \quad E_k \in \mathbb{R}^{\tilde{m} \times \tilde{m}} \quad (10)$$

where E_k is a randomly generated orthogonal matrix.

Experiments

Common settings and evaluation scheme

This section outlines the experimental settings and evaluation methods employed. The performance of DC-QE was compared against CA and individual analysis (IA). CA represents the ideal scenario where all raw data of users can be shared, including all covariates $X = [X_1, X_2, \dots, X_c]$, treatments $Z = [Z_1, Z_2, \dots, Z_c]$, and outcomes $Y = [Y_1, Y_2, \dots, Y_c]$, enabling a comprehensive estimation of treatment effects. However, IA estimated treatment effects using only the dataset owned by a single user due to privacy constraints. Specifically, IA used only covariates X_k , treatment Z_k , and outcome Y_k associated with user k .

The experiments were designed to verify whether DC-QE outperformed IAs and provided results comparable to those achieved through CA. We created pseudo-user groups by partitioning the data in

two ways to simulate the data distribution: IID and non-IID partitioning. Details of these partitioning methods are provided in subsequent sections.

Each experiment employed the bootstrap method to randomly sample all data samples and estimate the treatment effect from the extracted datasets. The number of bootstrap repetitions B was fixed at 100 due to computational limitations. We note that the bootstrap method in these experiments involves sampling from the population under study and should not be conflated with the bootstrap-based dimensionality reduction technique used by individual users to construct intermediate representations. Logistic regression was used to estimate propensity scores, while caliper matching was applied for the matching process.

The parameters used in DC-QE were set as follows: Anchor data were generated by random sampling from a uniform distribution bounded by the minimum and maximum values of each covariate. The sample size of the anchor data was defined as $r = \sum_{k=1}^c n_k$. The dimension of the intermediate and collaborative representations was configured as $\tilde{m} = \hat{m} = m - 1$.

Experiments were conducted with the following three combinations for the dimensions generated using the bootstrap-based method \tilde{m}_{BS} and those created through dimensionality reduction \tilde{m}_{DR} : $(\tilde{m}_{DR}, \tilde{m}_{BS}) = (\tilde{m}, 0), (\frac{\tilde{m}}{2}, \frac{\tilde{m}}{2}), (0, \tilde{m})$. Logistic regression was employed for bootstrap-based construction, while PCA was used for dimensionality reduction. These configurations evaluated the performance of DC-QE under bootstrap-based dimensionality reduction.

The evaluation metrics included inconsistency, maximum absolute standardized mean difference (MASMD), and gap, with additional metrics for non-IID distributions, such as maximum absolute Jeffreys divergence (MJD), to assess whether the distribution after matching approximated the true distribution. Smaller values for these metrics indicated better performance. Each evaluation metric is explained below.

Accuracy of estimated treatment effect

Significant deviation between the estimated treatment effect and the true value indicates the ineffectiveness of the algorithm. Therefore, we used the gap method to measure the deviation between estimated treatment effects and those obtained through CA. The Gap is calculated as:

$$Gap(\hat{\tau}, \hat{\tau}^{CA}) = \sqrt{\frac{1}{B} \sum_{b=1}^B (\hat{\tau}_b - \hat{\tau}_b^{CA})^2} \quad (11)$$

where B represents the number of bootstrap iterations, while $\hat{\tau} = [\hat{\tau}_1, \hat{\tau}_2, \dots, \hat{\tau}_B]$ and $\hat{\tau}^{CA} = [\hat{\tau}_1^{CA}, \hat{\tau}_2^{CA}, \dots, \hat{\tau}_B^{CA}]$ denote the estimated treatment effects obtained during each bootstrap iteration.

Inconsistency of estimated propensity score

Propensity scores play a critical role in propensity score matching. Significant deviations between estimated propensity scores and their true values result in suboptimal matching performance. Inconsistency was evaluated by comparing the propensity scores from CA ($\hat{e}^{CA} = [\hat{e}_1^{CA}, \hat{e}_2^{CA}, \dots, \hat{e}_n^{CA}]$) with scores obtained in the experiments ($\hat{e} = [\hat{e}_1, \hat{e}_2, \dots, \hat{e}_n]$) as follows:

$$Inconsistency(\hat{e}, \hat{e}^{CA}) = \sqrt{\frac{1}{n} \sum_{i=1}^n (\hat{e}_i - \hat{e}_i^{CA})^2} \quad (12)$$

Covariate balance

Matching aimed to balance covariates between treatment and control groups, making covariate balance an essential evaluation metric. The standardized mean difference (SMD) is commonly used for this purpose[32] and is expressed as:

$$d_{cont}^j = \frac{\bar{x}_T^j - \bar{x}_C^j}{\sqrt{(s_T^j + s_C^j)/2}}, \quad d_{bin}^j = \frac{\hat{p}_T^j - \hat{p}_C^j}{\sqrt{(\hat{p}_T^j(1 - \hat{p}_T^j) + \hat{p}_C^j(1 - \hat{p}_C^j))/2}} \quad (13)$$

where d_{cont}^j and d_{bin}^j represent the SMDs for continuous and binary covariates j -th, respectively. \bar{x}_T^j and \bar{x}_C^j denote the mean covariate j in the treatment and control groups, respectively. Similarly, \bar{s}_T^j and \bar{s}_C^j

represent the corresponding standard deviations, while \hat{p}_T^j and \hat{p}_C^j denote the proportions of covariate j equal to 1 in the treatment and control groups, respectively.

We evaluated covariate balance using the MASMD, which is defined as the maximum absolute value of the SMDs across all covariates, as expressed in equation (14):

$$MASMD(\mathbf{d}) = \max_j |d^j| \quad (14)$$

where $\mathbf{d} = [d_{cont}^1, \dots, d_{cont}^{m_{cont}}, d_{bin}^1, \dots, d_{bin}^{m_{bin}}]$.

Distribution similarity between two-groups

The distribution obtained after matching may not accurately reflect the true distribution in non-IID settings, where the covariate distributions of data differ across users. While MASMD effectively evaluates the covariate balance between treatment and control groups, it does not measure the fidelity of the distribution post-matching. Therefore, assessing the alignment between the covariate distribution and the true distribution after matching is crucial. Jeffreys Divergence[33], a symmetrized version of the Kullback-Leibler divergence, was employed to evaluate the similarity between the two distributions:

$$D_j(P^j \| P_{CA}^j) = KL(P^j \| P_{CA}^j) + KL(P_{CA}^j \| P^j) \quad (15)$$

$$KL(P^j \| P_{CA}^j) = \sum_{b=1}^{bins} p^j(b) \log \frac{p^j(b)}{p_{CA}^j(b)} \quad (16)$$

where P^j and P_{CA}^j represent the probability distributions of covariate j . The variable “bins” denotes the number of intervals in the probability distribution, set to 20 for this experiment. We evaluated the Jeffreys Divergence using its maximum value, as follows:

$$MJD = \max_j D_j(P^j \| P_{CA}^j) \quad (17)$$

Moreover, we assumed that the covariate distribution obtained under the CA setting was the true distribution for experimental purposes because the true distribution was unknown.

Data partitioning

The data-partitioning methods are explained for both IID and non-IID settings. Data in the IID configuration were randomly divided into 50 parts, simulating a scenario with 50 users (e.g., small hospitals). The performance of DC-QE was evaluated with varying numbers of collaborating users (2, 5, 10, 30, and 50). Experimental results for each case were compared with those from IA and CA.

Data partitioning in a non-IID scenario was designed to simulate three hospitals, employing the following methods:

- **Quantity:** Data were partitioned such that each user held 20%, 30%, or 50% of the total data, allocated randomly.
- **Label ratio:** Data were divided such that each user held an equal number of samples, with the proportion of treatment group samples for each user constituting 0.5%, 1%, or 2% of the total data samples.
- **Cluster:** Data were grouped into three clusters using uniform manifold approximation and projection and k-means clustering based on data covariates.

Performance evaluations for IA, CA, and DC-QE were compared in all non-IID scenarios. Notably, cluster-based partitioning is expected to result in more substantial covariate distribution differences across institutions compared with the quantity and label ratio methods because it is driven by covariate characteristics.

Result

Matching result

A specific example is presented in Table 2 to demonstrate the reduction in covariate bias achieved through DC-QE matching. It shows the SMDs pre- and post-matching. This example involves an

experiment where allopurinol was used as the treatment. The DC-QE results correspond to the scenario in which PCA was employed to generate the intermediate representation, and collaboration occurred across all users. While this is a single example, comparisons between IA and CA are provided in subsequent sections. Table 2 indicates that matching with DC-QE reduced bias to a certain extent.

Table 2. Matching example of DC-QE. Data are presented as mean (std).

Sample size	unit	Before matching n=10197			After matching (DC-QE) n=234		
		Control	Treatment	SMD	Control	Treatment	SMD
Diuretic	-	0.003 (0.057)	0.065 (0.248)	0.346	0.043 (0.203)	0.051 (0.222)	0.04
Beta-adrenergic antagonist	-	0.017 (0.128)	0.14 (0.349)	0.473	0.068 (0.253)	0.094 (0.293)	0.094
Renin-angiotensin system inhibitor	-	0.018 (0.133)	0.178 (0.384)	0.558	0.205 (0.406)	0.222 (0.418)	0.042
Antipurine	-	0.001 (0.03)	0.019 (0.136)	0.182	0.026 (0.159)	0.026 (0.159)	0
Alkalizer	-	0.017 (0.13)	0.047 (0.212)	0.168	0.026 (0.159)	0.034 (0.182)	0.05
Nonsteroidal anti-inflammatory drug	-	0.026 (0.158)	0.084 (0.279)	0.259	0.111 (0.316)	0.111 (0.316)	0
Aspirin	-	0.001 (0.031)	0.019 (0.136)	0.18	0.009 (0.092)	0.009 (0.092)	0
Corticosteroid	-	0.042 (0.2)	0.121 (0.328)	0.294	0.171 (0.378)	0.179 (0.385)	0.022
Colchicine	-	0.0 (0.014)	0.0 (0.0)	-0.02	0.0 (0.0)	0.0 (0.0)	-
CKD stage	-	2.069 (1.092)	3.056 (1.106)	0.898	3.051 (1.049)	3.051 (1.121)	0
High-density lipoprotein cholesterol	mg/dl	50.889 (12.33)	49.073 (13.813)	-0.139	49.874 (12.093)	49.462 (13.965)	-0.031
Hemoglobin A1c	%	6.044 (1.146)	6.028 (1.08)	-0.015	5.906 (0.66)	5.841 (0.881)	-0.083
eGFR	g/dl	86.603 (49.982)	46.719 (28.571)	-0.98	47.481 (25.145)	47.256 (29.746)	-0.008
Albumin	mg/dl	3.837 (0.676)	3.79 (0.726)	-0.067	3.883 (0.757)	3.913 (0.65)	0.042
Creatinine	mg/dl	1.013 (1.413)	1.896 (2.248)	0.47	1.654 (1.903)	1.77 (1.992)	0.06
Triglycerides	mg/dl	125.427 (91.417)	150.71 (101.225)	0.262	155.222 (134.693)	146.479 (91.511)	-0.076
Serum uric acid	mg/dl	5.087 (1.773)	6.007 (2.322)	0.445	6.153 (2.012)	5.88 (2.498)	-0.12
Age	-	58.086 (17.471)	65.57 (13.366)	0.481	63.744 (13.141)	64.41 (15.014)	0.047
Sex	-	0.524 (0.499)	0.159 (0.367)	-0.835	0.179 (0.385)	0.145 (0.354)	-0.093
Hemoglobin	g/dl	12.592 (2.255)	12.428 (2.593)	-0.068	12.84 (2.716)	12.552 (2.788)	-0.105
Urine pH	-	6.499 (0.601)	6.35 (0.793)	-0.211	6.376 (0.576)	6.423 (0.803)	0.067
Urine occult blood	-	0.441 (1.058)	0.495 (1.022)	0.052	0.436 (1.012)	0.47 (0.952)	0.035

IID setting

The experimental outcomes for the IID settings are depicted in Fig. 2. The three graphs on the left display the metrics (Gap, Inconsistency, and MASMD) for experiments where allopurinol served as the treatment, while the three graphs on the right illustrate the results for febuxostat. DC-QE, in collaboration with all users (50 hospitals), outperformed IA across all three metrics (see Fig. 2). Additionally, the performance of DC-QE improved with an increasing number of collaborating users, approaching the ideal performance of CA. The configuration $(\tilde{m}_{DR}, \tilde{m}_{BS}) = (21,0)$ delivered the highest overall performance in terms of creating the intermediate representation. Conversely, the configuration $(\tilde{m}_{DR}, \tilde{m}_{BS}) = (0,21)$ resulted in significantly poor MASMD compared with $(\tilde{m}_{DR}, \tilde{m}_{BS}) = (21,0)$ and $(11,10)$.

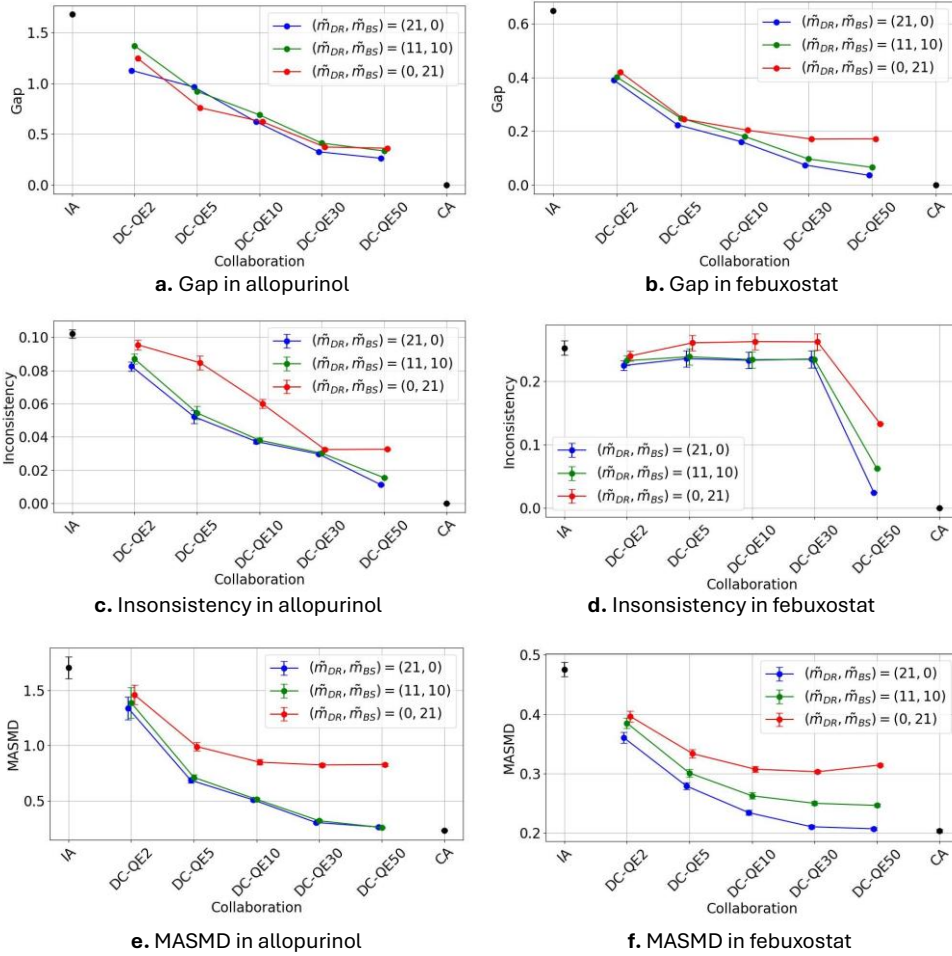


Fig. 2. Simulation results for the IID settings (left: allopurinol; right: febuxostat).

Non-IID setting

The experimental results for the non-IID setting under three data partitioning methods are presented in Figures 3, 4, and 5: Fig.3 for quantity-based partitioning, Fig.4. for label-ratio partitioning, and Fig. 5 for cluster-based partitioning. IA $_i$ in these figures represents i -th user. Figures 3, 4, and 5 show that DC-QE outperformed IAs across most metrics. However, certain cases demonstrated instances where IA values surpassed those of DC-QE. For example, Figure 5 shows that the inconsistency for IA2 in the allopurinol experiment was lower than that of DC-QE for $(\tilde{m}_{DR}, \tilde{m}_{BS}) = (0, 21)$. Similarly, the MASMD values for IA1, IA2, and IA3 for febuxostat exceeded those of DC-QE with $(\tilde{m}_{DR}, \tilde{m}_{BS}) = (11, 10)$.

Identifying the optimal method for creating intermediate representations in non-IID settings was challenging. The quality-based partitioning in an experiment involving allopurinol and febuxostat experiments frequently yielded better results when for $(\tilde{m}_{DR}, \tilde{m}_{BS}) = (21, 0)$. However, configurations such as $(\tilde{m}_{DR}, \tilde{m}_{BS}) = (0, 21)$ and $(11, 10)$ occasionally achieved the best scores for label-ratio and cluster-based partitioning. Notably, the configuration $(\tilde{m}_{DR}, \tilde{m}_{BS}) = (0, 21)$ produced the best results across all the metrics in the cluster-based febuxostat experiment (Fig. 5).

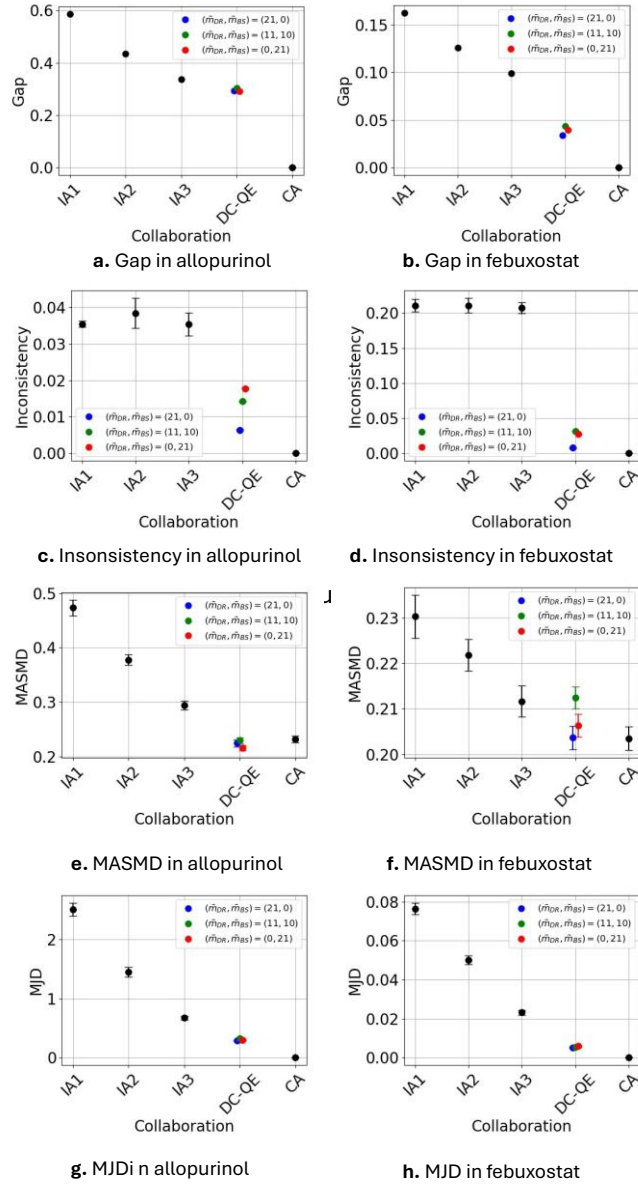


Fig. 3. Simulation results for the non-IID setting with quantity-based partitioning (left: allopurinol; right: febuxostat).

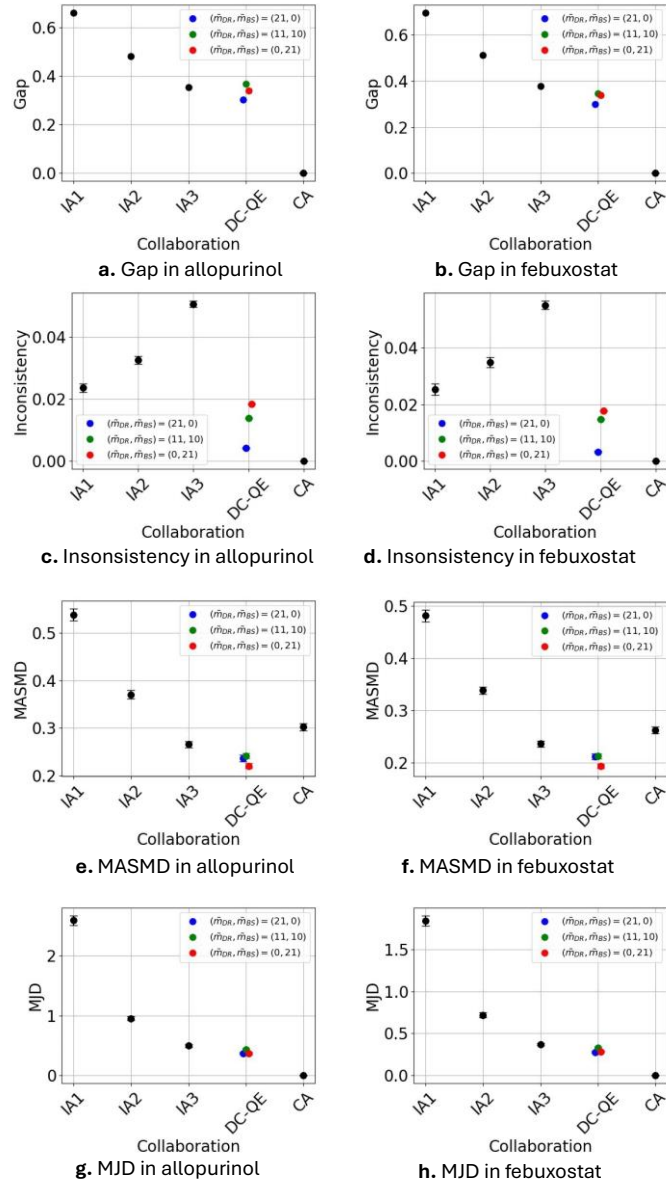


Fig. 4. Simulation results for the non-IID setting with label ratio-based partitioning (left: allopurinol; right: febuxostat).

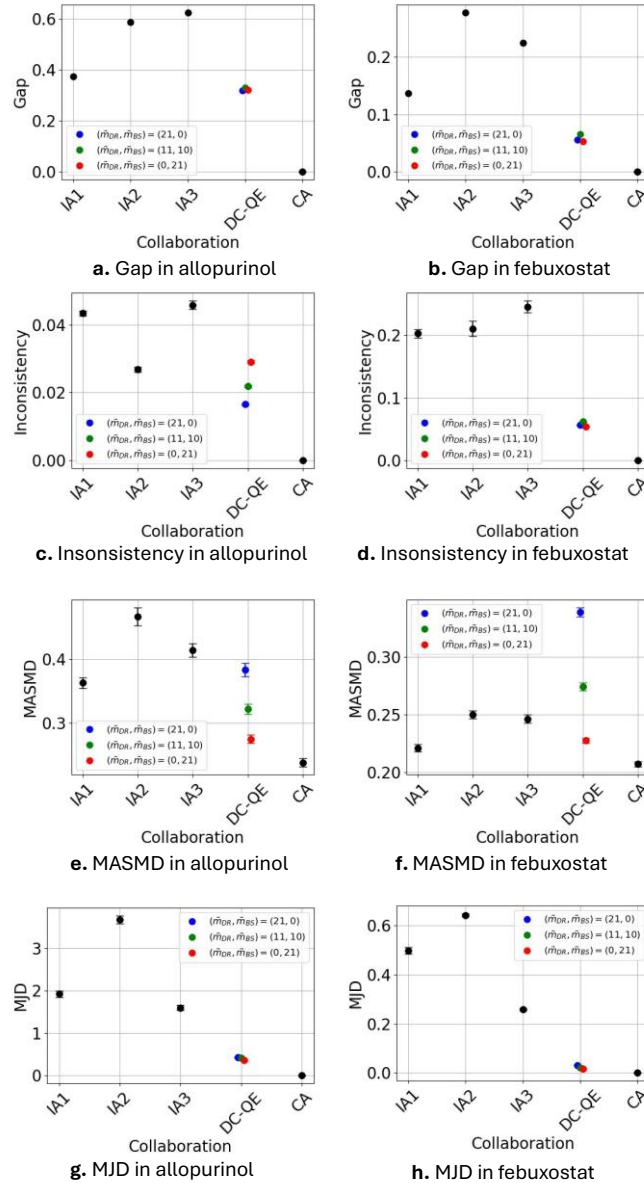


Fig. 5. Simulation results for the non-IID setting with cluster-based partitioning (left: allopurinol; right: febuxostat).

Discussion

This section discusses the results of the numerical experiments from two perspectives: the performance of DC-QE relative to IA and CA and the influence of intermediate representation methods on DC-QE performance.

Collaboration in DC-QE demonstrated superior performance over IA. The results closely approximated those of CA when all user data were included in the collaboration. Performance enhancements were evident even with minimal collaboration, as observed in the IID setting with only two users (Fig. 2). Moreover, improvements in IAs were also observed in non-IID settings (Figures 3, 4, and 5). These findings indicate that DC-QE exhibits robustness to medical data. Notably, performance gains were achieved even when individual users possessed small datasets (see the IID setting, DC-QE2). It suggests the potential utility of DC-QE is estimating treatment effects for rare diseases with limited case data.

Although the MASMD for IA1 in the febuxostat experiment was lower than that of DC-QE, IA1 exhibited a large MJD, indicating substantial deviation from the CA distribution (Fig. 5). However, DC-QE with $(\tilde{m}_{DR}, \tilde{m}_{BS}) = (0, 21)$ achieved small MJD values and MASMD < 0.25 , confirming its superior metrics. These observations affirm that DC-QE performs better than IA in non-IID settings.

DC-QE exhibited the highest performance in the IID setting when the intermediate representations were generated using $(\tilde{m}_{DR}, \tilde{m}_{BS}) = (21, 0)$. However, this configuration did not consistently yield the best results in non-IID settings. For example, in the febuxostat experiments under cluster-based partitioning, the highest performance was observed with $(\tilde{m}_{DR}, \tilde{m}_{BS}) = (0, 21)$.

Cluster partitioning in non-IID settings resulted in the most divergent covariate distributions. When PCA was used to create intermediate representations, differences in the transformation matrix axes across institutions likely caused significant information loss in collaborative representations. However, the bootstrap-based method (BS axes) effectively approximated the solution space subspace, resulting in superior performance in non-IID settings. These results suggest that increasing the number of BS axes could maintain DC-QE performance in the case of significantly divergent covariate distributions. A detailed analysis of this approach will be undertaken in future research.

Conclusion

This study demonstrated the application of DC-QE, a technique enabling integrated analysis and causal inference for distributed areas while preserving privacy, to medical datasets. Additionally, a dimensionality reduction method tailored for DC-QE was proposed and evaluated using various reduction strategies.

Experiments confirmed that DC-QE performs effectively in both IID and non-IID scenarios. Bootstrap-based dimensionality reduction proved beneficial in maintaining performance under conditions where covariate distributions varied substantially across users.

DC-QE outperformed IA even with datasets as small as 100 samples per user, highlighting its applicability in collaborative medical data analysis involving hospitals with limited data. DC-QE enables the identification of previously unknown causal relationships, such as those relevant to drug repositioning or therapeutic interventions for rare diseases, by facilitating privacy-preserving collaboration.

Future work will explore extending the DC analysis framework by combining DC-QE with survival analysis[31] to estimate hazard ratios while addressing bias. Achieving this would further enhance the utility of the DC framework in medical research by combining privacy preservation with robust bias elimination and hazard ratio estimation.

Data availability

The datasets used in this study were obtained from the University of Tsukuba Hospital and are subject to restrictions. These data were accessed under license for the current study and Japanese Act on the Protection of Personal Information, and so is not publicly available. Interested researchers may request access to the data from the corresponding author upon reasonable request and approval from the University of Tsukuba Hospital.

Acknowledgments

The authors express their gratitude to the University of Tsukuba Hospital for providing the medical data. This study was partially funded by the Cross-ministerial Strategic Innovation Promotion Program (SIP) on the “Integrated Health Care System” Grant (JPJ012425), the Japan Science and Technology Agency (JST) (Nos. No. JPMJPF2017, JPMJPR23I3 (PRESTO)), Japan Society for the Promotion of Science (JSPS), and

the Grants-in-Aid for Scientific Research (JP23H03502). The authors would like to thank Editage (www.editage.jp) for English language editing.

Author contributions

T. N., Y. K., A. T., and Y. O. designed the study. T. N. conducted data processing and analysis. T. N., Y. K., A. T. and Y. O. wrote the manuscript. Y. K., A. I., and T. S. constructed a DC analysis model tailored to the current problem set and interpreted the results mathematically. M. S. and R. T. obtained the data from the University of Tsukuba Hospital. R. K., R. T., and K. Y. assisted in validating the analysis from a medical standpoint and interpreting the results. All the authors have read and approved the final version of the manuscript.

- [1]. Farjat, A. E. *et al.* The importance of the design of observational studies in comparative effectiveness research: Lessons from the GARFIELD-AF and ORBIT-AF registries. *Am. Heart J.* **243**, 110–121 (2022).
- [2]. Bärnighausen, T. *et al.* Quasi-experimental study designs series-paper 4: Uses and value. Quasi-Experimental Study Designs Series—paper 4. *J. Clin. Epidemiol.* **89**, 21–29 (2017).
- [3]. Ligthelm, R. J. *et al.* Importance of observational studies in clinical practice. *Clin. Ther.* **29**, 1284–1292 (2007).
- [4]. Wang, Y.-R. & Tsai, Y.-C. The protection of data sharing for privacy in financial vision. *Appl. Sci.* **12**, 7408 (2022).
- [5]. Simpson, E. *et al.* Understanding the barriers and facilitators to sharing patient-generated health data using digital technology for people living with long-term health conditions: A narrative review. *Front. Public Health* **9**, 641424 (2021).
- [6]. El Emam, K., Rodgers, S. & Malin, B. Anonymising and sharing individual patient data. *BMJ* **350**, h1139–h1139 (2015).
- [7]. Hulsen, T. Sharing is Caring-Data sharing initiatives in healthcare. *Int. J. Environ. Res. Public Health* **17**, 3046 (2020).
- [8]. McMahan, B., Moore, E., Ramage, D., Hampson, S. & Arcas, B. A. y. Communication-efficient learning of deep networks from decentralized data in *Proceedings of the 20th International Conference on Artificial Intelligence and Statistics 1273–1282 (PMLR, 2017)*.

- [9]. Rieke, N. *et al.* The future of digital health with federated learning. *npj Digit. Med.* **3**, 119 (2020).
- [10]. Ashish Rauniyar *et al.* Federated learning for medical applications: A taxonomy, current trends, challenges, and future research directions, *Ar5iv*. <https://ar5iv.labs.arxiv.org/html/2208.03392>.
- [11]. Crowson, M. G. *et al.* A systematic review of federated learning applications for biomedical data. *PLOS Digit. Health* **1**, e0000033 (2022).
- [12]. Prayitno, *et al.* A systematic review of federated learning in the healthcare area: From the perspective of data properties and applications. *Appl. Sci.* **11**, 11191 (2021).
- [13]. Imakura, A. & Sakurai, T. Data collaboration analysis framework using centralization of individual intermediate representations for distributed data sets. *ASCE ASME J. Risk Uncertainty Eng. Syst. A* **6** (2020).
- [14]. Uchitachimoto, G. *et al.* Data collaboration analysis in predicting diabetes from a small amount of health checkup data. *Sci. Rep.* **13**, 11820 (2023).
- [15]. Kawamata, Y., Motai, R., Okada, Y., Imakura, A. & Sakurai, T. Collaborative causal inference on distributed data. *Expert Syst. Appl.* **244**, 123024 (2024).
- [16]. Rosenbaum, P. R. & Rubin, D. B. The central role of the propensity score in observational studies for causal effects. *Biometrika* **70**, 41–55 (1983).
- [17]. Zeng, R. *et al.* Associations of proton pump inhibitors with susceptibility to influenza, pneumonia, and COVID-19: Evidence from a large population-based cohort study. *eLife* **13**, RP94973 (2024).
- [18]. Hsu, Y.-C. *et al.* Comparing lenvatinib/pembrolizumab with Atezolizumab/Bevacizumab in unresectable hepatocellular carcinoma: A real-world experience with propensity score matching analysis. *Cancers* **16**, 3458 (2024).
- [19]. Yang, Q. *et al.* Ischemic cardio-cerebrovascular disease and all-cause mortality in Chinese elderly patients: A propensity-score matching study. *Eur. J. Med. Res.* **29**, 330 (2024).
- [20]. Chuang, M.-H. *et al.* New-onset obstructive airway disease following COVID-19: A multicenter retrospective cohort study. *BMC Med.* **22**, 360 (2024).

- [21]. Chou, H.-W. *et al.* Comparative effectiveness of allopurinol, febuxostat and benzbromarone on renal function in chronic kidney disease patients with hyperuricemia: A 13-year inception cohort study. *Nephrol. Dial. Transplant.* **33**, 1620–1627 (2018).
- [22]. Becker, M. A. *et al.* Febuxostat compared with allopurinol in patients with hyperuricemia and gout. *N. Engl. J. Med.* **353**, 2450–2461 (2005).
- [23]. Bruce S. P. Febuxostat: A Selective Xanthine Oxidase Inhibitor for the Treatment of Hyperuricemia and Gout - Susan P Bruce, 2006. *The Annals of pharmacotherapy* **40**, 2187–2194 (2006).
- [24]. Hosoya, T, Sasaki, T. & Ohashi, T. Clinical efficacy and safety of topiroxostat in Japanese hyperuricemic patients with or without gout: a randomized, double-blinded, controlled phase 2b study. *Clin. Rheumatol.* **36**, 649–656 (2017).
- [25]. Matsuo, S. *et al.* Revised equations for estimated GFR from serum creatinine in Japan. *Am. J. Kidney Dis.* **53**, 982–992 (2009).
- [26]. Imakura, A., Inaba, H., Okada, Y. & Sakurai, T. Interpretable collaborative data analysis on distributed data. *Expert Syst. Appl.* **177**, 114891 (2021).
- [27]. Imakura, A., Kihira, M., Okada, Y. & Sakurai, T. Another use of SMOTE for interpretable data collaboration analysis. *Expert Syst. Appl.* **228**, 120385 (2023).
- [28]. Wold, S., Esbensen, K. & Geladi, P. Principal component analysis. *Chemom. Intell. Lab. Syst.* **2**, 37–52 (1987).
- [29]. Fisher, R. A. The use of multiple measurements in taxonomic problems. *Ann. Eugen.* **7**, 179–188 (1936).
- [30]. He, X. & Niyogi, P. Locality preserving projections in *Adv. Neural Inf. Process. Syst.* (MIT Press, 2003) **16**.
- [31]. Imakura, A., Tsunoda, R., Kagawa, R., Yamagata, K. & Sakurai, T. DC-COX: Data collaboration Cox proportional hazards model for privacy-preserving survival analysis on multiple parties. *J. Biomed. Inform.* **137**.

- [32]. Austin, P. C. & Stuart, E. A. Moving towards best practice when using inverse probability of treatment weighting (IPTW) using the propensity score to estimate causal treatment effects in observational studies. *Stat. Med.* **34**, 3661–3679 (2015).
- [33]. Jeffreys, H. An invariant form for the prior probability in estimation problems. *Proc. R. Soc. Lond. A Math. Phys. Sci.* **186**, 453–461 (1946).

Figure legends

- Fig. 1.** Preprocessing flowchart, where n indicate the number of samples.
- Fig. 2.** Simulation results for the IID settings (left: allopurinol; right: febuxostat).
- Fig. 3.** Simulation results for the non-IID setting with quantity-based partitioning (left: allopurinol; right: febuxostat).
- Fig. 4.** Simulation results for the non-IID setting with label ratio-based partitioning (left: allopurinol; right: febuxostat).
- Fig. 5.** Simulation results for the non-IID setting with cluster-based partitioning (left: allopurinol; right: febuxostat).